



Prediction of Response to Neoadjuvant Chemoradiotherapy by MRI-Based Machine Learning Texture Analysis in Rectal Cancer Patients

Sajad P. Shayesteh¹ · Afsaneh Alikhassi² · Farshid Farhan^{3,4} · Reza Gahletaki⁴ · Masume Soltanabadi⁵ · Peiman Haddad^{3,4} · Ahmad Bitarafan-Rajabi^{6,7}

Published online: 27 August 2019

© The Author(s) 2019

Abstract

Introduction Neoadjuvant chemoradiotherapy (nCRT) followed by surgical resection is the standard treatment for locally advanced rectal cancer (LARC). Radiomics can be used as noninvasive biomarker for prediction of response to therapy. The main aim of this study was to evaluate the association of MRI texture features of LARC with nCRT response and the effect of Laplacian of Gaussian (LoG) filter and feature selection algorithm in prediction process improvement.

Methods All patients underwent MRI with a 3T clinical scanner, 1 week before nCRT. For each patient, intensity, shape, and texture-based features were derived from MRI images with LoG filter using the IBEX software and without preprocessing. We identified responder from a non-responder group using 9 machine learning classifiers. Then, the effect of preprocessing LoG filters with 0.5, 1 and 1.5 value on these classification algorithms' performance was investigated. Eventually, classification algorithm's results were compared in different feature selection methods.

Result Sixty-seven patients with LARC were included in the study. Patients' nCRT responses included 11 patients with Grade 0, 19 with Grade 1, 26 with Grade 2, and 11 with Grade 3 according to AJCC/CAP pathologic grading. In MR Images which were not preprocessed, the best performance was for Ada boost classifier (AUC = 74.8) with T2W MR Images. In T1W MR Images, the best performance was for ada boost classifier (AUC = 78.1) with a $\sigma = 1$ preprocessing LoG filter. In T2W MR Images, the best performance was for naive Bayesian network classifier (AUC = 85.1) with a $\sigma = 0.5$ preprocessing LoG filter. Also, performance of machine learning models with CfsSubsetEval (CF SUB E) feature selection algorithm was better than others.

Conclusion Machine learning can be used as a response predictor model in LARC patients, but its performance should be improved. A preprocessing LoG filter can improve the machine learning methods performance and at the end, the effect of feature selection algorithm on model's performance is clear.

Keywords MRI · Rectal cancer · Radiomics · Machine learning

The scientific guarantor of this publication is Ahmad Bitarafan Rajabi.

✉ Peiman Haddad
haddad@tums.ac.ir

✉ Ahmad Bitarafan-Rajabi
bitarafan@hotmail.com

Sajad P. Shayesteh
shayeste_sajad@yahoo.com

¹ Department of Physiology, Pharmacology and Medical Physics, Faculty of Medicine, Alborz University of Medical Sciences, Karaj, Iran

² Department of Radiology, Cancer Institute of Iran, Tehran University of Medical Sciences, Tehran, Iran

³ Radiation Oncology Research Center, Cancer Institute, Tehran University of Medical Sciences, Tehran, Iran

⁴ Radiation Oncology Department, Cancer Institute, Tehran University of Medical Sciences, Tehran, Iran

⁵ Department of Nuclear Medicine, Faculty of Medicine, Shahrekord University of Medical Sciences, Shahrekord, Chaharmahal and Bakhtiari, Iran

⁶ Cardiovascular Intervention Research Center, Rajaie Cardiovascular Medical and Research Center, Iran University of Medical Sciences, Tehran, Iran

⁷ Echocardiography Research Center, Rajaie Cardiovascular Medical and Research Center, Iran University of Medical Sciences, Tehran, Iran

Introduction

Colorectal cancer (CRC) is the third most common cancer worldwide, the second leading cause of cancer deaths in 2016 in the USA and is slightly more common in men. Rectal cancer accounts for one-third of all colorectal cancers and approximately 39,220 new cases of rectal cancer with an estimated 5-year overall survival rate of 65% occur each year [1–5]. Nowadays, nCRT followed by surgical resection is the standard treatment, which is widely used for treatment of locally advanced (cT3, 4 and/or N+) rectal cancer (LARC) [6, 7]. Prediction of response to treatment has a significant role in selection of treatment approach. Response to nCRT is an important prognostic factor but significantly varies among patients [8].

Prediction of the response to nCRT would be useful in LARC patient, but qualitative evaluation of response to treatment by medical images is not possible in early phase, because qualitative evaluation is performed by monitoring tumor anatomical characteristics, including length, area, and tumor volume, which are not apparent in early phases during therapy [9, 10]. Preprocessing is an important step in medical imaging, which is useful for improving quality, viewing of image details and increasing diagnostic accuracy by image enhancement, edge detection, noise reduction, etc. Filtering is usually applied in preprocessing, which is done by the Laplacian of Gaussian (LoG) filter. This filter highlights features at different scales, by two functions, including the Gaussian and the Laplacian function, for filtering and differentiation respectively. Low filter values is applied for highlighting fine anatomic details and high filter values is used for enhancing coarse anatomic details. Some studies have used different values of LoG filter in medical imaging of cancerous patients for better prediction of response process [9–11].

In a large number of high-throughput medical image features, radiomics are helpful to predict tumor behavior during therapy, providing accurate, noninvasive, and reliable biomarker for prediction of response to treatment [12, 13]. Feature selection algorithms are used for determination of relevant features to avoid over-fitting, resulted from more sample numbers compared with derived feature numbers, providing more accurate models. Quantitative texture analysis and data mining methods have been used as predictive and prognostic biomarkers in multiple cancers, including lung, breast, head and neck, and prostate cancer [14–18].

Machine learning (ML) is a programmable method, applied as predictive and prognostic models for radiomics which can “learn” using the data to improve response prediction. There are many different ML models for this purpose, which should be evaluated to determine the most useful model [19–21].

In this study, we aimed to investigate different ML algorithms on radiomic features extracted from rectal MRI to find best predictive models. Also, the effects of LoG filter and feature selection algorithms on LMs predictive performance were studied.

Methods

Figure 1 shows the different steps of our study in the format of overall framework. Below the different phases of study are outlined.

Patient Characteristics

This study is retrospective, including 67 patients (44 male and 23 female) referred to Imam Khomeini hospital, Tehran University of medical science from October 2016 to April 2018. This study was approved by the Ethics Committee of Iran University of Medical Science (ethics approval no. K17-137) and informed consent was acquired from all patients. Inclusion criteria were the location of tumor within 15 cm above anal verge, tumor penetration to perirectal fat (cT3–4) or lymph node involvement, age \leq 80 years, WHO performance status of 0–2, normal CBC, liver and renal function tests, and lack of any prior treatment for the disease. All patients received concurrent nCRT. They received 45–46 Gy external beam radiation in 23–25 fractions with 18 MV photons to the tumor and loco regional disease including pre-sacral and internal iliac lymph nodes with a boost to the tumor for a total of 50–50.4 Gy, concurrent capecitabine at 825 mg/m² twice daily. The exclusion criterion is as follows: patients with previous radiation therapy and/or chemotherapy for rectal cancer were excluded from study.

Image Acquisition

All images were acquired on a 3.0-T MRI system (Tesla-Trio, Siemens Healthcare, Germany) 1 week before nCRT. A 32-channel pelvic phased array coil was used for signal reception. MRI protocol included axial, sagittal, and coronal T1-weighted images (TR 400 m/s, TE 17 m/s, FOV 20_20 mm, matrix 256_256, slice thickness of 3 mm with 1 mm gap) and axial, sagittal, and coronal T2-weighted images (TR 3000 m/s, TE 110 m/s, FOV 20_20 mm, matrix 256_256, slice thickness of 3 mm with 1 mm gap).

Tumor Segmentation

Gross tumor volume was drawn around the rectal tumor, by two readers: a 10-year experience radiation oncologist, and a 15-year experience radiologist using a designated multi-

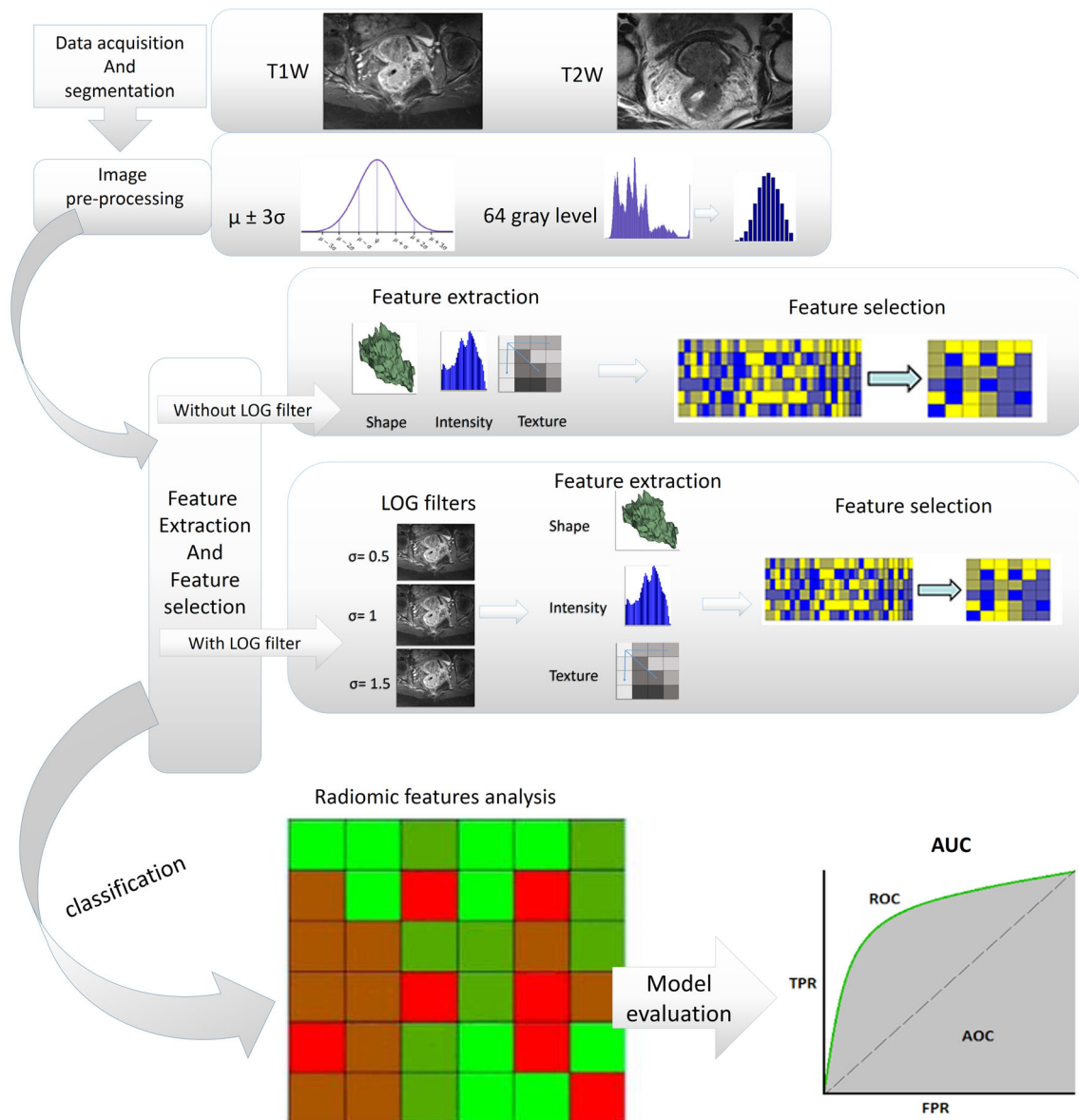


Fig. 1 Overall framework of study

platform, free, and open source software package for visualization and medical image computing (3D slicer, version 4.8.1; available at: <http://slicer.org/>). All slices were reviewed, followed by drawing on the T1W and T2W images. Tumor segmentation was performed on each MR image, creating a volume of interest (VOI).

Preprocessing and texture feature extraction Pre-processing and discretization to 64 Gy level were done by a method proposed by Collewet et al. for noise reduction, intensity normalization, and discretization. In this method, all image intensities are normalized between $\mu \pm 3\sigma$, where μ is the mean value of gray levels inside the region of interest (ROI), and σ is the standard deviation [22, 23].

Also, feature extraction was applied on T1W and T2W MR Images with and without preprocessing filters in order to evaluate the filter effect on radiomic model performance. The filters include the LoG filter with sigma 0.5, 1, and 1.5. For feature extraction, we used the freely available radiomic software, imaging biomarker explorer (IBEX) that runs in Matlab platform.

Various radiomic features from different feature sets including intensity, shape-, and texture-based features were extracted from processed and un-processed T1W and T2W MR images. Extracted features included shape features ($n = 17$), intensity histogram features ($n = 9$), intensity direct ($n = 19$), neighbor intensity difference ($n = 5$), co-occurrence matrix features (COM) ($n = 19$), and gray level run-length matrix features (GLRLM) ($n = 11$) [9, 24].

Response Assessment For all patients, surgery was done 4–8 weeks after nCRT. After inking, the specimens were fixed in formalin for 24 h. The whole tumor and mesorectum were serially sliced, axially, at 3 mm intervals, and treatment response was assessed according to the 4-category American Joint Committee on Cancer and College of American Pathologists (AJCC/CAP). The TRG according to AJCC/CAP was established as follows: grade 0 (pathologic response complete, PCR) is defined as no viable cancer cell; grade 1 (moderate response) means single cells or small groups of cancer cells; grade 2 (minimal response) are residual cancer outgrown by fibrosis; and grade 3 (poor response) is fibrosis outgrown by residual cancer [25–27].

Univariate Radiomic Analysis For univariate analysis, significant radiomic features correlated with response were selected and a logistic regression classifier was used to find their predictive performance (based on AUC). Also, these features were compared between responder and non-responder groups. A paired *t* test was performed to assess the significance of the differences between two groups. Statistical significance was assumed if $p < 0.05$ and all reported *p*-values are two-sided.

Multivariate Radiomic Analysis Statistical analyses were performed using the WEKA software version 3.8 (University of Waikato, Hamilton, New Zealand) [28]. Patients were divided into either the responder (Grade 0 or Grade 1) or non-responder (Grade 2 or Grade 3) group according to according to AJCC/CAP pathologic grading. We identify responder from a non-responder group by using 9 classifiers, including Bayesian Network, naive Bayesian network, Ada boost M1, iterative classifier optimizer, logit boost, randomizable filtered classifier, random sub space, random forest, and K logistic model tree (LMT). Then, effect of preprocessing LoG filters with 0.5, 1, and 1.5 values on these classification algorithms' performance is investigated. For all of machine learning

models the CfsSubsetEval (CF SUB E) feature selection algorithm was used. We compare model performance with the validation AUC using the 10-fold cross validation (CV).

Feature Selection

Feature selection is the process of finding the most meaningful features, variables, and predictors for use in model construction. When the number of derived features is more than the number of samples, there is a danger of over-fitting analyses, and must be reduced by feature reduction [18, 29]. In this study, we investigate the effect of different feature selection techniques on classification performance using the WEKA software version 3.8 (University of Waikato, Hamilton, New Zealand). In the classifiers performance investigation with and without LoG filters, all of classifiers have the best performance in T2W MR Images with $\sigma = 0.5$. So, we investigate the effect of six different feature selection algorithms on classification model's performance in T2W MR Images with $\sigma = 0.5$. The feature selection algorithms and their definition were shown on Table 1.

Result

Patients and Response

Sixty-seven patients (44 men; mean age, 60.01 years; age range, 31–80 years; 23 women; mean age, 52.2 years; age range, 27–67 years) with LARC were included in the study. All patients underwent simultaneous nCRT, followed by surgery. Patients' CRT responses included 11 patients with Grade 0, 19 with Grade 1, 26 with Grade 2, and 11 with Grade 3 according to AJCC/CAP pathologic grading. Patient data and their response grade were shown in Table 2.

Table 1 Feature selection algorithms

| Feature selection method | Definition |
|--|---|
| Cfs Subset Eval (CF SUB E) | Evaluates the worth of a subset of attributes by considering the individual predictive ability of each feature along with the degree of redundancy between them. |
| Correlation Attribute Eval (CO AT EV) | Evaluates the worth of an attribute by measuring the correlation (Pearson's) between it and the class. |
| Gain Ratio Attribute Eval (GA FA AT) | Evaluates the worth of an attribute by measuring the gain ratio with respect to the class. |
| One R Attribute Eval (One R AT) | Evaluates the worth of an attribute by using the One R classifier. |
| Relief F Attribute Eval (RE F AT) | Evaluates the worth of an attribute by repeatedly sampling an instance and considering the value of the given attribute for the nearest instance of the same and different class. |
| Symmetrical Uncert Attribute Eval (SYM AT) | Evaluates the worth of an attribute by measuring the symmetrical uncertainty with respect to the class. |

Table 2 Patient characteristics

| Demographics | Frequency <i>N</i> | Percent % |
|--------------|--------------------|-----------|
| Gender | | |
| Male | 44 | 65.7 |
| Female | 23 | 34.3 |
| Total | 67 | 100 |
| Age | | |
| 18–40 | 15 | 22.4 |
| 41–60 | 23 | 34.3 |
| > 61 | 29 | 43.3 |
| Total | 67 | 100 |
| Response | | |
| Grade 0 | 11 | 9.4 |
| Grade 1 | 19 | 26.4 |
| Grade 2 | 26 | 47.2 |
| Grade 3 | 11 | 17 |

Texture Analysis

Radiomic features with high correlation to therapy response were selected for T1W and T2W MR images separately. Our univariate analysis showed that nine and 11 radiomic features have high correlation with nCRT response for T1W and T2W MR Image's respectively. For T1W MR images, we found that three of the top radiomic features are from gray level co-occurrence matrix (GLCOM), two of them from gray level run length matrix (GLRLM) and four of them from intensity base feature set. For T2W MR Images, we found that all 11 top radiomic features are from co-occurrence matrix (COM) feature set. The results on AUC logistic regression classifier for these feature are shown in Fig. 2.

In T1W MR images, max probability has the best performance (AUC, 0.61/CI 0.55–0.66, *p* value 0.0004) followed by percentile (AUC, 0.60/CI 0.54–0.66, *p* value 0.0013), long-run high gray-level (AUC, 0.59/CI 0.53–0.61, *p* value 0.0031), inverse diff moment norm (AUC, 0.58), and percentile area (AUC, 0.57). In T2W MR images, dissimilarity has the best performance (AUC, 0.65/CI 0.58–0.71, *p* value, 0.0001), followed by Sum Average (AUC, 0.64/CI 0.58–0.70, *p* value, 0.0003), inter-quartile range (AUC, 0.63/CI 0.55–0.68, *p* value 0.0023), cluster tendency (AUC, 0.63), variance (AUC, 0.63), and cluster prominence (AUC, 0.61).

Based on these results in responder and non-responder groups, significant difference exists among selected radiomic features between two groups in TW1 and T2W MR images, but there is no significant difference between two groups in all features (*p* value > 0.05).

For multivariate radiomic analysis, our results were shown in Table 3. For ML classifiers performance investigation, BN and iterative classifier optimizer classifiers with AUC 0.64 (CI 0.57–0.68, *p* value 0.0003) and 0.72 (CI 0.61–0.77, *p* value

0.0001) was found as high predictive model for un-processed T1W and T2W MR Features respectively.

Our result on pre-processed images showed that the LoG filter improves the classifiers performance. Results on pre-processed images with $\sigma = 0.5$, we also showed that random sub space (AUC, 59.1; CI 0.52–0.63, *p* value 0.0013) naive Bayesian network (AUC, 85.1, CI 0.77–0.89, *p* value 0.0001) classifiers have more predictive roles for T1W and T2W MR images respectively. In preprocessing with $\sigma = 1$, random sub space (AUC, 79.3, CI 0.75–0.83, *p* value 0.0023) and naive randomizable filtered classifier (AUC, 68.8) are the best predictive models for T1W and T2W MR images respectively. Also, results on pre-processed images with $\sigma = 1.5$, showed that randomizable filtered classifier (AUC, 68 CI 0.62–0.74, *p* value 0.0002) and naive Bayesian network (AUC, 80.6, CI 0.77–0.84, *p* value 0.0001) classifiers are the best predictive models for T1W and T2W MR Images respectively.

Feature Selection Performance

In the last phase, the best result of LoG filters in T1w and T2w MR images is selected and the effect of different feature selection algorithms on mentioned classifiers performance is investigated. Almost the best performance was for T2w MR images with a fine (0.5) LoG filter. For effect of different feature selection algorithm analyses, our results were shown in Table 4. The best performance was for CF SUB E algorithm with a naive Bayesian network classifier (AUC, 85.1) followed by Ada boost M1 (AUC, 79.4), Logit Boost (AUC, 79.3), and K logistic model tree (AUC, 77.5). After CF SUB E feature selection algorithm the best performance was for SYM AT algorithm with logit boost classifier (AUC, 74.5).

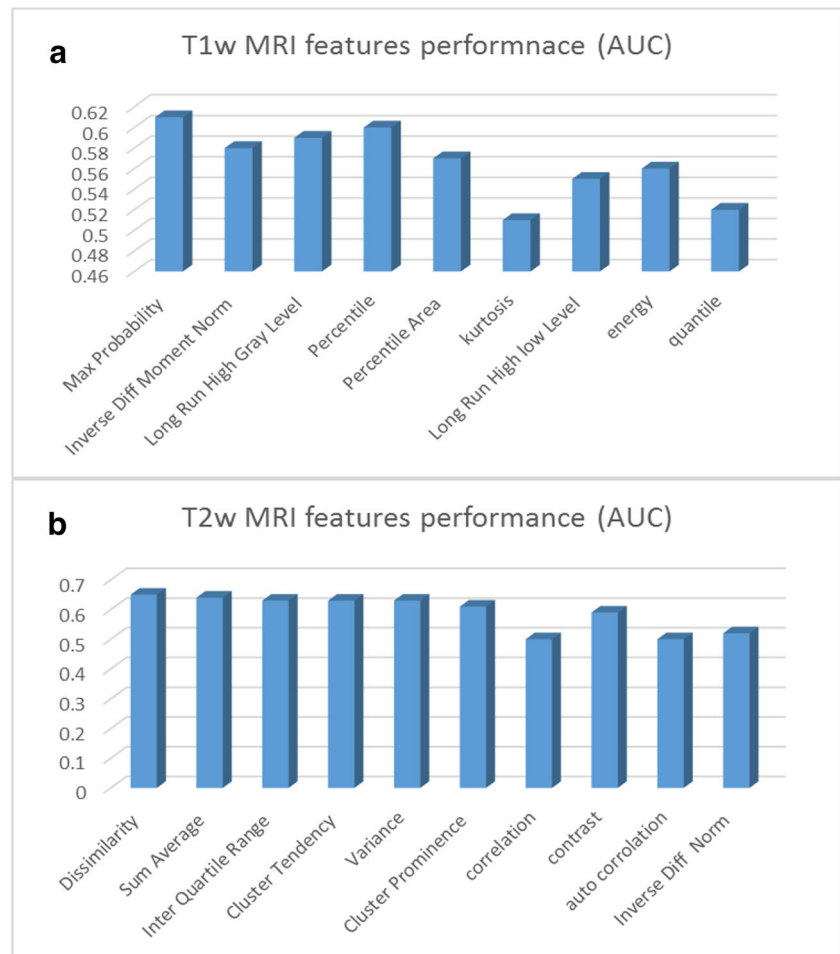
Discussion

In oncology, imaging has a fundamental role, providing valuable data for cancer management. MRI is a noninvasive imaging modality, producing three-dimensional images, without ionizing radiation and better contrast and spatial resolution [30].

Radiomics, extracting and mining large number of quantitative and distinct medical imaging features, is a new field in medical imaging, which hypothesizes that some quantitative and distinct imaging features provide crucial information regarding tumor phenotype with clinical significance in different diseases, providing valuable data for personalized therapy [13, 31].

Our study demonstrated that quantitative features from Computerized Texture Analysis of LARC at Pretreatment T1w and T2w MR Imaging have correlation with response to nCRT and can be used as noninvasive biomarker for prediction of response to treatment. ML methods are reliable and

Fig. 2 Features with high correlation ability to predict nCRT response in LARC in **a** T1W MR images. **b** T2W MR images



accurate predictors and preprocessing LoG filter can improve their performance. In the majority of classifiers, performance of features derived from T2w was better than T1w MR images [32, 33].

Previous studies have shown the feasibility of radiomic modeling in LARC. Nie et al. using artificial neural network as classifier found that radiomic features extracted from T1/T2W, diffusion-weighted (DW) and dynamic contrast-enhanced (DCE) MR images could enhance the predictive power of pathologic response after preoperative nCRT for LARC [34]. In another study, Meng et al. used MRI texture analysis for nCRT response prediction and found several textures such as standard deviation (SD), kurtosis, and energy; and uniformity were statistically different between responder and non-responder groups [35]. Horvat N et al. used MR images to compare value of T2W radiomic textures compared with qualitative assessment at T2W and DW imaging for diagnosis of clinical complete response in patients with LARC after nCRT. They used random forest for classification and they found better performance of T2W-based radiomic features compared with qualitative assessment at T2-W and DW imaging for diagnosing pCR in patients with LARC after nCRT [36].

LoG filter is the combination of a Gaussian smoothing operator with a kernel of standard deviation (σ) followed by an isotropic Laplacian filter, which uses to highlight image details at various scales. In this study performance of ML methods improved by LoG filter in T2w and T1w MR images. Chee CG et al. used CT images without filtration and with LoG spatial filter with various filter values (1.0, 1.5, 2.0, and 2.5) to evaluate the association of texture features of LARC patients with nCRT response and disease-free survival (DFS). They found that responder group showed significantly lower entropy, higher uniformity, and lower standard deviation in no filtration and fine (1.0) and medium (1.5) LoG filter values than the non-responder group [9]. Also, Dinapoli N et al. used MR images with multiple σ of LoG filter to predict pCR probability using only pre-treatment MR images in LARC patients. They found that, only pre-treatment MR imaging can be helpful for predicting pCR probability in LARC patients [37].

The feature selection algorithm can identify relevant and robust features to improve model's performance and avoid overfitting. At the last phase, we investigate the effect of six different feature selection algorithms (Table 1) on

Table 3 AUC of texture feature analysis in different LoG filter values

| | Classifiers | | | | | | | | |
|--------------|------------------|------------------------|--------------|--------------------------------|-------------|----------------------------------|------------------|---------------|-----------------------|
| | Bayesian network | Naive bayesian network | Ada boost M1 | Iterative classifier optimizer | Logit boost | Randomizable filtered classifier | Random sub space | Random forest | K logistic model tree |
| T1W | Filter value | | | | | | | | |
| | No filtration | 63.9 | 51.2 | 50.0 | 51.0 | 51.2 | 52.2 | 51.3 | 50.0 |
| | 0.5 (fine) | 52.3 | 54.2 | 56.8 | 58.1 | 53.8 | 59.1 | 55.3 | 50.0 |
| | 1 (medium) | 56.2 | 68.0 | 78.1 | 70.3 | 78.1 | 79.3 | 53.1 | 52.9 |
| T2W | 1.5 (coarse) | 52.1 | 50.0 | 51.2 | 51.2 | 52.1 | 51.3 | 50.0 | 50.0 |
| | Filter value | | | | | | | | |
| | No filtration | 66.7 | 51.1 | 74.8 | 71.8 | 63.4 | 60.5 | 54.3 | 51.1 |
| | 0.5 (fine) | 72.5 | 85.1 | 79.4 | 81.3 | 79.3 | 72.3 | 71.8 | 61.5 |
| 1 (medium) | 57.6 | 65.0 | 58.9 | 58.6 | 60.2 | 55.2 | 56.2 | 50.0 | |
| 1.5 (coarse) | 57.6 | 80.6 | 80.1 | 53.6 | 80.1 | 67.1 | 66.4 | 60.9 | |

Table 4 AUC of different feature selection algorithms in fine (sigma 0.5) LoG filter

| Feature selection | Classifiers | | | | | | | | |
|-----------------------------------|------------------|------------------------|-------------|--------------------------------|-------------|----------------------------------|------------------|---------------|-----------------------|
| | Bayesian network | Naive Bayesian network | Adaboost M1 | Iterative classifier optimizer | Logit Boost | Randomizable filtered classifier | Random sub space | Random forest | K logistic model tree |
| Cifs Subset Eval | 72.5 | 85.1 | 79.4 | 81.3 | 79.3 | 66.2 | 72.3 | 71.8 | 77.5 |
| Correlation Attribute | 61.2 | 57.8 | 73.1 | 55.9 | 75.6 | 72.0 | 55.7 | 51.6 | 58.8 |
| Gain Ratio Attribute Eval | 56.2 | 52.7 | 73.1 | 58.4 | 74.8 | 62.6 | 55.7 | 52.0 | 59.7 |
| One R Attribute Eval | 56.2 | 55.1 | 73.9 | 59.0 | 74.8 | 64.1 | 50.2 | 55.1 | 58.8 |
| Relief F Attribute Eval | 57.3 | 52.7 | 72.0 | 54.1 | 75.9 | 59.3 | 51.6 | 52.7 | 58.8 |
| Symmetrical Uncert Attribute Eval | 65.3 | 54.8 | 73.2 | 55.3 | 74.5 | 66.4 | 56.5 | 55.4 | 66.8 |

prediction process. Our results demonstrate that feature selection algorithm can affect the ML model's performance and the best result was for CF SUB E algorithm. Megherbi et al. investigated the effect of clinical feature selection on surgery outcome predictions and as like as our study, they found effect of feature selection algorithm on ML performance [18, 38]. In another study, Saeys Y et al. investigated the necessity of applying feature selection techniques. They found that the main problem in the bioinformatics domain is the large input dimensionality, with the small sample sizes, and to deal with these problems, a wealth of feature selection techniques has been designed [18].

Although our results are significant, this study suffers from some limitations. First is the small sample size of 53 patients. Further studies with a large patient data are warranted to verify our results. Second is feature robustness and reproducibility. Based on several studies, radiomic feature are vulnerable against some challenges including image acquisition, reconstruction, segmentation, and processing. Although our data acquisition was same for all patients, there is a challenge on tumor segmentation. Third is classifier model validation. We used 10-fold cross validation which is proposed by several studies, but external validation with a large train data may improve the results.

Conclusion

In conclusion, ML can be used as a response predictor model in LARC patients, but its performance should be improved. Effect of coarse preprocessing LoG filter on ML performance is better than fine filters and at the end, effect of feature selection algorithm on model's performance is clear.

Funding The author(s) received no financial support for the research, authorship, and/or publication of this article.

Compliance with Ethical Standards

Conflict of Interest The authors declare that they have no conflict of interest.

Statistics and Biometry All authors kindly provided statistical advice for this manuscript.

Informed Consent Not applicable. Retrospective study.

Ethical Approval Institutional Review Board approval was obtained.

Methodology Retrospective.

Diagnostic or prognostic study/experimental Multicenter study.

Open Access This article is distributed under the terms of the Creative Commons Attribution 4.0 International License (<http://creativecommons.org/licenses/by/4.0/>), which permits unrestricted use, distribution, and reproduction in any medium, provided you give appropriate credit to the original author(s) and the source, provide a link to the Creative Commons license, and indicate if changes were made.

References

1. Birkman EM, et al. Protein phosphatase 2A (PP2A) inhibitor CIP2A indicates resistance to radiotherapy in rectal cancer. *Cancer Med*. 2018.
2. Cossio DC, et al. Polymorphism of the Cox-2 gene and susceptibility to colon and rectal cancer. *Arq Bras Cir Dig*. 2017;30(2):114–7.
3. Hathout L, Williams TM, Jabbour SK. The impact of novel radiation treatment techniques on toxicity and clinical outcomes in rectal cancer. *Curr Colorectal Cancer Rep*. 2017;13(1):61–72.
4. Siegel RL, Miller KD, Jemal A. Cancer statistics, 2016. *CA Cancer J Clin*. 2016;66(1):7–30.
5. Martinez-Useros J, Moreno I, Fernandez-Aceñero MJ, Rodriguez-Remirez M, Borrero-Palacios A, Cebrian A, et al. The potential predictive value of DEK expression for neoadjuvant chemoradiotherapy response in locally advanced rectal cancer. *BMC Cancer*. 2018;18(1):144.
6. Zhang C, et al. Morphologic predictors of pathological complete response to neoadjuvant chemoradiotherapy in locally advanced rectal cancer. *Oncotarget*. 2018;9(4):4862–74.
7. Sathyakumar K, Chandramohan A, Masih D, Jesudasan MR, Pulimood A, Eapen A. Best MRI predictors of complete response to neoadjuvant chemoradiation in locally advanced rectal cancer. *Br J Radiol*. 2016;89(1060):20150328.
8. Noh GT, Kim NK. Genomic predictor of complete response after chemoradiotherapy in rectal cancer. *Ann Transl Med*. 2016;4(24):493.
9. Chee CG, Kim YH, Lee KH, Lee YJ, Park JH, Lee HS, et al. CT texture analysis in patients with locally advanced rectal cancer treated with neoadjuvant chemoradiotherapy: a potential imaging biomarker for treatment response and prognosis. *PLoS One*. 2017;12(8):e0182883.
10. Sun Y-S, et al. Locally advanced rectal carcinoma treated with preoperative chemotherapy and radiation therapy: preliminary analysis of diffusion-weighted MR imaging for early detection of tumor histopathologic downstaging. *Radiology*. 2009;254(1):170–8.
11. Anand A, Tripathy SS, Kumar RS. An improved edge detection using morphological Laplacian of Gaussian operator. In *Signal Processing and Integrated Networks (SPIN)*, 2015 2nd International Conference on. 2015. IEEE.
12. Chicklore S, Goh V, Siddique M, Roy A, Marsden PK, Cook GJR. Quantifying tumour heterogeneity in 18F-FDG PET/CT imaging by texture analysis. *Eur J Nucl Med Mol Imaging*. 2013;40(1):133–40.
13. Aerts HJ, et al. Decoding tumour phenotype by noninvasive imaging using a quantitative radiomics approach. *Nat Commun*. 2014;5:4006.
14. Sacconi B, Anzidei M, Leonardi A, Boni F, Saba L, Scipione R, et al. Analysis of CT features and quantitative texture analysis in patients with lung adenocarcinoma: a correlation with EGFR mutations and survival rates. *Clin Radiol*. 2017;72(6):443–50.
15. Nie K, Chen JH, Yu HJ, Chu Y, Nalcioglu O, Su MY. Quantitative analysis of lesion morphology and texture features for diagnostic prediction in breast MRI. *Acad Radiol*. 2008;15(12):1513–25.

16. Ailianou A, Mundada P, de Perrot T, Puzstaszieri M, Poletti PA, Becker M. MRI with DWI for the detection of posttreatment head and neck squamous cell carcinoma: why morphologic MRI criteria matter. *Am J Neuroradiol*. 2018;39:748–55.
17. Schieda N, Lim CS, Idris M, Lim RS, Morash C, Breau RH, et al. MRI assessment of pathological stage and surgical margins in anterior prostate cancer (APC) using subjective and quantitative analysis. *J Magn Reson Imaging*. 2017;45(5):1296–303.
18. Saeys Y, Inza I, Larrañaga P. A review of feature selection techniques in bioinformatics. *Bioinformatics*. 2007;23(19):2507–17.
19. Parmar C, et al. Radiomic machine-learning classifiers for prognostic biomarkers of head and neck cancer. *Front Oncol*. 2015;5:272.
20. Cruz JA, Wishart DS. Applications of machine learning in cancer prediction and prognosis. *Cancer Informat*. 2006;2:117693510600200030.
21. Kotsiantis SB, Zaharakis I, Pintelas P. Supervised machine learning: a review of classification techniques. *Emerging artificial intelligence applications in computer engineering*. 2007;160:3–24.
22. Molina D, Pérez-Beteta J, Martínez-González A, Martino J, Velásquez C, Arana E, et al. Influence of gray level and space discretization on brain tumor heterogeneity measures obtained from magnetic resonance images. *Comput Biol Med*. 2016;78:49–57.
23. Vallières M, et al. A radiomics model from joint FDG-PET and MRI texture features for the prediction of lung metastases in soft-tissue sarcomas of the extremities. *Phys Med Biol*. 2015;60(14):5471–96.
24. Ng F, Ganeshan B, Kozarski R, Miles KA, Goh V. Assessment of primary colorectal cancer heterogeneity by using whole-tumor texture analysis: contrast-enhanced CT texture as a biomarker of 5-year survival. *Radiology*. 2013;266(1):177–84.
25. Haddad P, Miraie M, Farhan F, Fazeli MS, Alikhassi A, Maddah-Safaei A, et al. Addition of oxaliplatin to neoadjuvant radiochemotherapy in MRI-defined T3, T4 or N+ rectal cancer: a randomized clinical trial. *Asia-Pacific Journal of Clinical Oncology*. 2017;13(6):416–22.
26. Edge SB, Compton CC. The American Joint Committee on Cancer: the 7th edition of the AJCC cancer staging manual and the future of TNM. *Ann Surg Oncol*. 2010;17(6):1471–4.
27. Nougaret S, Fujii S, Addley HC, Bibeau F, Pandey H, Mikhael H, et al. Neoadjuvant chemotherapy evaluation by MRI volumetry in rectal cancer followed by chemoradiation and total mesorectal excision: initial experience. *J Magn Reson Imaging*. 2013;38(3):726–32.
28. Singhal S, Jena M. A study on WEKA tool for data preprocessing, classification and clustering. *Int J Innov Technol Exploring Eng*. 2013;2(6):250–3.
29. Gillies RJ, Kinahan PE, Hricak H. Radiomics: images are more than pictures, they are data. *Radiology*. 2015;278(2):563–77.
30. Moffat BA, Chenevert TL, Lawrence TS, Meyer CR, Johnson TD, Dong Q, et al. Functional diffusion map: a noninvasive MRI biomarker for early stratification of clinical brain tumor response. *Proc Natl Acad Sci U S A*. 2005;102(15):5524–9.
31. Parmar C, Grossmann P, Bussink J, Lambin P, Aerts HJWL. Machine learning methods for quantitative radiomic biomarkers. *Sci Rep*. 2015;5:13087.
32. Davnall F, Yip CSP, Ljungqvist G, Selmi M, Ng F, Sanghera B, et al. Assessment of tumor heterogeneity: an emerging imaging tool for clinical practice? *Insights Imaging*. 2012;3(6):573–89.
33. De Cecco CN, et al. Texture analysis as imaging biomarker of tumoral response to neoadjuvant chemoradiotherapy in rectal cancer patients studied with 3-T magnetic resonance. *Investig Radiol*. 2015;50(4):239–45.
34. Nie K, Shi L, Chen Q, Hu X, Jabbour SK, Yue N, et al. Rectal cancer: assessment of neoadjuvant chemoradiation outcome based on radiomics of multiparametric MRI. *Clin Cancer Res*. 2016;22(21):5256–64.
35. Meng Y, et al. MRI texture analysis in predicting treatment response to neoadjuvant chemoradiotherapy in rectal cancer. *Oncotarget*. 2018;9(15):11999.
36. Horvat N, Veeraraghavan H, Khan M, Blazic I, Zheng J, Capanu M, et al. MR imaging of rectal cancer: radiomics analysis to assess treatment response after neoadjuvant therapy. *Radiology*. 2018;287(3):833–43.
37. Dinapoli N, et al. Magnetic resonance, vendor-independent, intensity histogram analysis predicting pathologic complete response after radiochemotherapy of rectal cancer. *Int J Radiat Oncol Biol Phys*. 2018.
38. Megherbi D, Soper B. Effect of feature selection on machine learning algorithms for more accurate predictor of surgical outcomes in benign pro static hyperplasia cases (BPH). In *Computational Intelligence for Measurement Systems and Applications (CIMSAS)*, 2011 IEEE International Conference on. 2011. IEEE.

Publisher's Note Springer Nature remains neutral with regard to jurisdictional claims in published maps and institutional affiliations.